DIGITAL ACCESS TO SCHOLARSHIP AT HARVARD
DASH.HARVARD.EDU

HARVARD LIBRARY

HER-2-Targeted Nanoparticle-Affibody Bioconjugates for Cancer Therapy

Citation
Published version
https://doi.org/10.1002/cmdc.200800122

Link
http://nrs.harvard.edu/urn-3:HUL.InstRepos:29005176

Terms of use
This article was downloaded from Harvard University's DASH repository, and is made available under the terms and conditions applicable to Other Posted Material (LAA), as set forth at
https://harvardwiki.atlassian.net/wiki/external/NGY5NDE4ZjgzNTc5NDQzMGIzZWZhMGFlOWI2M2EwYTg

Accessibility
https://accessibility.huit.harvard.edu/digital-accessibility-policy

Share Your Story
The Harvard community has made this article openly available.
Please share how this access benefits you. Submit a story

NIH Public Access
Author Manuscript
ChemMedChem. Author manuscript; available in PMC 2012 December 05.

Published in final edited form as:
ChemMedChem. 2008 December ; 3(12): 1839–1843. doi:10.1002/cmdc.200800122.

HER-2 Targeted Nanoparticle-Affibody Bioconjugates for Cancer Therapy

Frank Alexis[a,b], **Pamela Basto**[a,b], **Etgar Levy-Nissenbaum**[a,b], **Aleksandar F. Radovic-Moreno**, **Liangfang Zhang**[b], **Eric Pridgen**[c], **Adrew Z. Wang**[b,d], **Shawn L. Marein**[a], **Katrina Westerhof**[a,b], **Linda K. Molnar**[e], and **Omid C. Farokhzad**[a,b]

[a] Department of Anaesthesiology Brigham Brigham and Women's Hospital and Harvard Medical School and Women's Hospital and Harvard Medical School 75 Francis St, Boston, MA 02115, USA 75 Francis St, Boston, MA 02115, USA

[b] Division of Health Science and Technology Massachusetts Institute of Techn Massachusetts Institute of Technology 77 Massachusetts Ave., Cambridge, MA 02139, USA

[c] Department of Chemical Engineering Massachusetts Institute of Technology Massachusetts Institute of Technology

[d] Department of Radiation Oncology Brigham and Women's Hospital and Harvard Medical School 75 Francis St, Boston, MA 02115, USA

[e] National Cancer Institute, National Institutes of Health, Bethesda, Maryland, 20892

Abstract

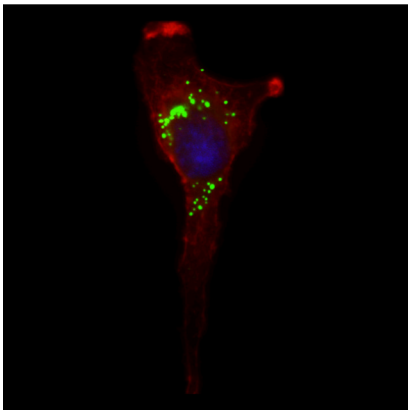

Affibodies are a class of polypeptide ligands that are potential candidates for cell- or tissue-specific targeting of drug-encapsulated controlled release polymeric nanoparticles (NPs). Here we report the development of drug delivery vehicles comprised of polymeric NPs that are surface modified with Affibody ligands that bind to the extracellular domain of the trans-membrane human epidermal growth factor receptor 2 (HER-2) for targeted delivery to cells which over express the HER-2 antigen. NPs lacking the anti-HER-2 Affibody did not show significant uptake by these cells. Using paclitaxel encapsulated NP-Affibody (1 wt% drug loading), we demonstrated increased cytotoxicity of these bioconjugates in SK-BR-3 and SKOV-3 cell lines. These targeted, drug encapsulated NPAffibody bioconjugates may be efficacious in treating HER-2 expressing carcinoma.

Fax: 617-730-2801 ofarokhzad@partners.org.

$watermark-text
$watermark-text
$watermark-text

Keywords

Affibody; nanoparticle; PLA/PEG; antitumor agents; targeted therapy

Drug encapsulated controlled release nanoparticles (NPs) have the potential to improve the current cancer chemotherapies by increasing drug efficacy, lowering drug toxicity, and maintaining a relatively high concentration of drug at the site of interest [1-3]. Encapsulating drugs within NPs can improve the solubility and pharmacokinetics of drugs, and, in some cases, enable the further clinical development of new chemical entities that have stalled because of poor pharmacokinetic properties. The breakthrough potential of cancer nanotechnology is becoming more apparent with several examples of non-targeted NP platforms in clinical practice today. These include Abraxane (paclitaxol-albumin) [4], Doxil (doxorubicin-liposomes) [5], DaunoXome (daunorubicin-liposomes)[6], Cyclosert (camptothecin-cyclodextrin) [7] and Genexol-PM [paclitaxolmethoxy-polyethyleneglycol-poly(D,L-Lactide)] [8]. The functionalization of non-targeted NPs with ligands that bind to the extracellular domain of tumor-associated trans-membrane antigens may further increase the therapeutic index of cytotoxic drugs by differentially targeting drugs to the diseases cells.

The first examples of targeted nanoparticles were reported in 1980 and despite nearly 3 decades of research, targeted nanoparticles have made a limited impact on human health. This is in part because the optimal biophysicochemical properties of the nanoparticles, including the choice of a suitable ligand for targeting has remained elusive [9-11]. These include the utilization of targeting approaches that go beyond antibodies which have several known drawbacks including their large hydrodynamic size which limits both intratumoral uptake and homogeneous distribution in the tumor adversely affecting pharmacokinetic properties. Further, the use of an antibody as a component of a multifunctional nanoparticle adds an additional level of complexity to the scale-up and manufacturing of the resultant targeted nanoparticles. There is a clear need for new methods of targeting that are compatible with the size of nanoparticles and their manufacturing. Additionally, while monoclonal antibodies have shown some promise their effects tend to be variable and ultimately not curative. Attempts to develop immunoconjugates, which add the therapeutic benefit of a drug, toxin, or radionuclide, have not met with much success either probably due to low drug content per antibody molecule. However, the combination of the targeting capabilities of an antibody, without the inherent limitations of antibodies [12] as mentioned above, and a controlled release system utilizing a payload consisting of a small molecule chemotherapeutic may prove to be advantageous.

The anti-HER-2 Affibody has many merits as a targeting ligand in contrast to an anti-HER-2 monoclonal antibody. Its small size (Molecular weight ~ 15 kDa) results in a favorable ratio of binding site to ligand size, bearing in mind that the molecular weight of an anti-HER-2 monoclonal antibody is typically about 150 kDa; it promotes an endocytosis dependent internalization mechanism [13-16]; it has a functional end group distanced from its active site for chemical conjugation; it has high *in vitro* and *in vivo* stability; and the total chemical synthesis allows facile large scale production of the Affibody. The anti-HER-2 Affibody (Z-HER2: 342 Affibody) has shown high binding affinity (k_D ~ 22 pM) to the recombinant extracellular domain of the protein HER-2 (HER-2-ECD) [17, 18]. In addition, Orlova et al. [17] has shown that this class of molecules can selectively bind to HER-2 over-expressing cell lines (SK-BR-3 and SK-OV-3). All of these characteristics make Affibody a potentially viable ligand for targeted drug delivery.

$watermark-text $watermark-text $watermark-text

$watermark-text

$watermark-text

$watermark-text

To develop HER-2 targeted drug encapsulated NPs, we conjugated the anti-HER-2 Affibody to the thiol-reactive maleimide of the PLA-PEG-Maleimide (PLA-PEG-Mal) copolymer of the previously formed NPs through a stable thioether bond and evaluated the targeting specificity and efficacy using fluorescent microscopy. Subsequently, we encapsulated paclitaxel into the targeted polymeric NPs and examined whether this system could increase the drug cytotoxicity in HER-2 positive cell lines: SK-BR-3 and SK-OV-3. We chose to deliver the taxane paclitaxel due to its poor water solubility which results in a reduced therapeutic index for intravenous administration of the free drug in a clinical setting.

We first synthesized a copolymer comprised of a hydrophobic block, poly ($_{D,L}$ lactic acid), and a hydrophilic block, poly(ethylene glycol) with a maleimide terminal group (PLA-PEG-Mal). Then the copolymers form negatively charged NPs with a core-shell structure in an aqueous environment via the nanoprecipitation method. The hydrophobic core of the NPs is capable of carrying pharmaceuticals, especially those with poor water solubility. The hydrophilic shell not only provides a “stealth” layer [19], together with the surface charge property (Zeta potential) = - 10 mV ± 5 mV) [20, 21], to improve the stability and the circulation half-time of these drug delivering NPs, but also functional maleimide groups for Affibody conjugation (Figure 1A). Lack of protein adsorption in solutions including 10%, 20% and 100% serum (data not shown) demonstrated the stability of NP size (< 100 nm). We also evaluated the freeze-drying process for storing the nanoparticles in a dry state, as described previously [22]. We were able to reconstitute nanoparticles with a similar original size after lyophilization, confirming the stability of this type of carrier to this process.

The anti-HER-2 Affibody molecule was previously selected against the extracellular domain of the HER-2 protein [23] and further modified by affinity maturation and dimerization [14, 18]. The anti-HER-2 Affibody is commercially available and has been shown to have high binding specificity and affinity *in vitro* and *in vivo* as a targeted imaging agent [17, 24-26]. Therefore, the multiple advantages of the combination of biodegradable polymeric NPs and targeting anti-HER-2 Affibody molecules led to our interest in developing a a targeted, controlled release drug delivery system for cancer therapy aimed at HER-2 positive cells. Particle size and surface charge (Zeta potential) of PLA-PEG-Mal NPs both with and without Affibody were characterized using laser light scattering, ZetaPALS system and electron microscopy (Figure 1A). The addition of Affibody molecules on the surface of the NPs did not significantly affect the size, size distribution and surface charge of the NPs (NP =70 ± 5nm, NP-Affibody 85 ± 5nm). The chemical conjugation of the Affibody molecules on the surface of the PLA-PEG-Mal NPs was confirmed using UV imaging (Figure 1A) and proton nuclear magnetic resonance spectroscopy in d-DMSO (^{1}H-NMR) (Figure 1B). To visualize the presence of Affibody molecules on the NPs, we labeled Affibody molecules with the fluorescence probe, Alexa Fluor 532, and subsequently conjugated them to the PLA-PEG-Mal NPs with different molar ratios of Affibody:PLA-PEG-Mal (0, 1, 2, 5, 20%). The NP-Affibody bioconjugates were then exposed under UV lamp to observe their fluorescence signals. As shown in Figure 1B, no fluorescence signal was observed from the NPs without fluorescently labeled Affibody, however, the fluorescence intensity from those NPs with fluorescent Affibody continuously enhances with the increase of Affibody:PLA-PEG-Mal molar ratio. The ^{1}H-NMR spectrum of the purified PLA-PEG-Affibody in d-DMSO showed the characteristic peaks of PLA-PEG at chemical shift of δ~ 1.4 ppm (–CH3 of the PLA backbone), δ ~ 3.6 ppm of (-CH2 of the PEG backbone) and δ~ 5.2 ppm (-CH of the PLA backbone) (Figure 1B). Additionally, we observed the characteristic peaks of the Affibody molecule in the chemical shift region of δ= 7-8 ppm that represents the amide bonds (NH-CO) within the Affibody polypeptide molecule. The NMR results suggest successful conjugation of the Affibody on the surface of PLA-PEG-Mal NPs.

$watermark-text

$watermark-text

$watermark-text

We next demonstrated the efficient binding and internalization of targeted NP-Affibody bioconjugates to HER-2 positive cancer cells using three cell lines: Capan-1 (Figure 2-B1), SK-BR-3 (Figure 2-B2), and SK-OV-3 (Figure 2-B3). After incubating NBD dye encapsulated NP-Affibody bioconjugates with the cells for 2 hr at 37°C and removing the excess bioconjugates, we observed a large amount of green dots in a punctuate pattern inside the targeted cells, suggesting an efficient targeting and internalization mechanism of the ~80 nm NP-Affibody bioconjugates to the HER-2 positive cells. In contrast, untargeted PLA-PEG NPs were slightly taken up by the cell lines after the same duration of incubation (Figure 2 A1-A3). To minimize cell passage effect on the observed results, this experiment was repeated four times with different cell passages and all of them gave the same observations. We also verified the cellular localization of the NP-Affibody bioconjugates using a z-axis scanning fluorescent microscopy and 3D image reconstitution. The rotated cross section of the 3D reconstitution images of a SK-BR-3 cell demonstrated the internalization of targeted NP-Affibody bioconjugates to the cell (Figure 3).

Orlova et al. [18] have shown the binding ability of Anti-HER-2 Affibody within 1 hr using immunofluorescence method. Our results are consistent with their findings and suggest a receptor mediated endocytosis mechanism. Internalization through an endocytosis mechanism has been previously described for anti-HER-2 monoclonal antibodies [27, 28] and is consistent with the kinetics of our targeted NPs entering the cells within 2 hours. Similarly, targeted drug delivery using RGD peptide sequences to integrins has also shown efficient binding and internalization in multiple types of cancers. In addition to efficient binding and internalization, the anti-HER-2 approach also offers improved cancer disease specificity with high affinity to HER-2 cell membrane receptors expressed in multiple types of cancers compared to RGD [29] .We prepared drug-containing and drug free Nps and targeted nanoparticles to evaluate their differential cytotoxicity using in vitro cell viability assay (MTS assays) with breast cancer and ovarian cancer cells (SK-BR-3; SK-OV-3), which over-express the HER-2 cell membrane receptors. In this study, we incubated various NP formulations with SK-BR-3 and SK-OV-3 cancer cells for 2 hours in optimem, washed cells with PBS to remove excess of NPs, and supplemented with fresh cell growth medium. We further incubated the cells for 3 days before using the MTS assay to quantify cell viability which was normalized to that of the cells in the absence of NPs.

The results showed that drug encapsulated targeted NPs had the highest cytotoxicity to both SK-BR-3 and SK-OV-3 cell lines; cell viability was 70 ± 5 % and 59 ± 5 %, respectively (Figure 4). The ANOVA test indicated that the cell viability of drug containing targeted NPs differed significantly from that of drug containing NPs ($p<0.05$). In contrast, free drug and NPs without encapsulated drugs are not toxic to both cell lines. These results are consistent with our previous studies using targeted NP-aptamer bioconjugates to deliver drugs to prostate cancer cells [30-33]. Therefore, this NP-Affibody bioconjugate system holds potential to be used as a biocompatible and biodegradable targeted drug delivery platform for multiple types of cancer therapeutics. Further, the modularity of the delivery system allows for tuning of the various parameters of the bioconjugates, such as NP size, surface charge and Affibody packing density, in order to optimize the drug delivery pharmacokinetics and its targeting efficiency for optimum specific therapeutic applications.

In summary, herein we report to our knowledge the first example of a targeted controlled release NP-Affibody bioconjugate for drug delivery to HER-2 positive cancer cells. Using FDA (Food Drug and Administration) approved polymers to form nanoparticles, we have demonstrated that the nanoparticle-Affibody bioconjugates were specifically and efficiently internalized to HER-2 positive cancer cells such as ovarian, breast and pancreatic cancer cells, thereby providing a promising way to deliver chemotherapeutic drugs to the cancer cells in a selective manner. This HER-2 targeted drug delivery platform can be tuned to

$watermark-text

$watermark-text

$watermark-text

encapsulate multiple types and combinations of drugs, increase drug loading, and optimize the surface coverage of the Affibody targeting ligands for specific therapeutic applications. Additional *in vivo* biodistribution and efficacy studies are needed to further evaluate the potential of the nanoparticle-Affibody bioconjugates for each therapeutic application as a systemic or locally administered drug delivery system.

Experimental Section

Nanoparticle characterization

Size (diameter) and Zeta-potential (surface charge) of NPs were evaluated by Quasi-elastic laser light scattering (QELS) using a ZetaPALS dynamic light-scattering detector (15 mW laser, incident beam = 676 nm; Brookhaven Instruments, Holtsville, NY). 200 μg of nanoparticles were dispersed in solution (~ 2ml) and measurements were performed in triplicate at room temperature.

Conjugation and Characterization of nanoparticle-Affibody bioconjugates

PLA-PEG-Mal polymeric NPs were incubated under stirring conditions with the Anti-HER-2 Affibody molecules (15kDa) at a molar ratio of Affibody:PLA-PEG-Mal of 5 % to form a stable bioconjugate. The NP-Affibody bioconjugates were purified to remove free Affibody molecules using Amicon Ultra centrifuge device (100 kDa molecular weight size exclusion). Subsequently, the thioether bond formation between the PLA-PEG-Mal NPs and the Affibody molecules was characterized using proton nuclear magnetic resonance (^{1}H-NMR, 600 MHz, Bruker Advance). Additionally, the chemical attachment of the fluorescent Affibody was confirmed using an Ultra Violet Imaging system (Kodak Electrophoresis Documentation and Analysis System 120). The Affibody molecule was fluorescently labeled with a red fluorescent probe, Alexa Fluor 532 (Invitrogen), purified and subsequently conjugated to PLA-PEG-Mal polymeric NPs at different molar ratios of Affibody:PLA-PEG-Mal ranging from 0 to 20 % (molar ratio). Then the purified NP-Affibody bioconjugate suspensions were imaged using a UV Kodak camera assisted with a red filter to show the visible effect of the fluorescent Affibody conjugated on non-fluorescent polymeric NPs.

Uptake assays of targeted and untargeted nanoparticles

The human ovarian adenocarcinoma (SK-OV-3; ATCC), human breast adenocarcinoma (SK-BR-3; ATCC), and human pancreatic adenocarcinoma (Capan-1, ATCC) were the HER-2 positive cell lines used for cytotoxicity and uptake efficacy studies of the NP-Affibody bioconjugates. HER-2 positive cell lines were grown in chamber slides (Cab-TekII, 8 wells; Nunc) within their growth medium (Modified McCoy's 5a (ATCC) supplemented with 100 units/ml aqueous penicillin G, 100 ug/ml streptomycin, and 10% FBS) to 70% confluence in 24 h (i.e., 50,000 cells/cm^2) in 5 % CO_2 incubator. On the day of the experiment, cells were washed with pre-warmed PBS and incubated with pre-warmed phenol-red–reduced OptiMEM media for 30 minutes, before adding 50 μg of NPs or NP-Affibody bioconjugates loaded with same amount of green fluorescent NBD dye (4-fluoro-7-nitrobenz-2-oxa-1,3-diazole). NP formulations were incubated with cells for 2 hours at 37°C, washed with PBS three times, fixed with 4% paraformaldehyde, blocked for 30 minutes at room temperature with 1 % BSA/PBS, permeabilized with 0.01 % Triton-X for 3 minutes, counterstained with Alexa-Fluor Phalloidin-Rhodamine (cytoskeleton staining), 4’,6-diamidino-2-phenylindole (DAPI, nucleus staining), mounted in fluorescence protecting imaging solution, and visualized using fluorescent microscopy (DeltaVision system; Olympus IX71). Digital images of green, red and blue fluorescence were acquired along the z-axis at 0.2 μm intervals using 60X oil immersion objective and DAPI, FITC and Rhodamine filters respectively. Images were overlaid, deconvoluted and 3D reconstruction was performed using Softwork software for acquisition and analysis.

$watermark-text

$watermark-text

$watermark-text

In vitro cellular toxicity assay of paclitaxel encapsulated into targeted and untargeted NPs

SK-BR-3 and SK-OV-3 were grown in 96-well plates at concentrations leading to 70% confluence in 24 h (i.e. 50,000 cells/cm^2). Defined amounts of paclitaxel were encapsulated into targeted and non-targeted nanoparticles (1 % wt/wt) and incubated with cell lines (5 ug Paclitaxel/well) in OptiMEM for two hours. Next, cells were washed and fresh media was supplemented. The cells were then allowed to grow for 72 hours and cell viability was assessed colorimetrically with MTS reagents (Invitrogen).

Supplementary Material

Refer to Web version on PubMed Central for supplementary material.

Acknowledgments

This work was supported by USA National Institutes of Health grant EB003647; and by a generous gift from Ms. Anne C. Gallo to BWH towards this research.

References

1. Farokhzad OC, Langer R. Advanced drug delivery reviews. 2006; 58(14):1456–1459. [PubMed: 17070960]
2. Langer R. Science (New York, N.Y. 2001; 293(5527):58–59.
3. Brigger I, Dubernet C, Couvreur P. Advanced drug delivery reviews. 2002; 54(5):631–651. [PubMed: 12204596]
4. Green MR, Manikhas GM, Orlov S, Afanasyev B, Makhson AM, Bhar P, Hawkins MJ. Ann Oncol. 2006; 17(8):1263–1268. [PubMed: 16740598]
5. Muggia FM. J Clin Oncol. 1998; 16(2):811–812. [PubMed: 9469384]
6. O'Byrne KJ, Thomas AL, Sharma RA, DeCatris M, Shields F, Beare S, Steward WP. British journal of cancer. 2002; 87(1):15–20. [PubMed: 12085249]
7. Schluep T, Hwang J, Cheng J, Heidel JD, Bartlett DW, Hollister B, Davis ME. Clin Cancer Res. 2006; 12(5):1606–1614. [PubMed: 16533788]
8. Lee KS, Chung HC, Im SA, Park YH, Kim CS, Kim SB, Rha SY, Lee MY, Ro J. Breast Cancer Res Treat. 2007
9. Alexis F, Rhee JW, Richie JP, Radovic-Moreno AF, Langer R, Farokhzad OC. Urologic oncology. 2008; 26(1):74–85. [PubMed: 18190835]
10. Pridgen EM, Langer R, Farokhzad OC. Nanomedicine (London, England). 2007; 2(5):669–680.
11. van Vlerken LE, Amiji MM. Expert opinion on drug delivery. 2006; 3(2):205–216. [PubMed: 16506948]
12. Pimm MV. Critical reviews in therapeutic drug carrier systems. 1988; 5(3):189–227. [PubMed: 3060267]
13. Dowsett M, Harper-Wynne C, Boeddinghaus I, et al. Cancer Res. 2001; 61(23):8452–8458. [PubMed: 11731427]
14. Kimura K, Sawada T, Komatsu M, et al. Clin Cancer Res. 2006; 12(16):4925–4932. [PubMed: 16914581]
15. Dowsett M, Harper-Wynne C, Boeddinghaus I, Salter J, Hills M, Dixon M, Ebbs S, Gui G, Sacks N, Smith I. Cancer research. 2001; 61(23):8452–8458. [PubMed: 11731427]
16. Kimura K, Sawada T, Komatsu M, Inoue M, Muguruma K, Nishihara T, Yamashita Y, Yamada N, Ohira M, Hirakawa K. Clin Cancer Res. 2006; 12(16):4925–4932. [PubMed: 16914581]
17. Orlova A, Magnusson M, Eriksson TL, et al. Cancer Res. 2006; 66(8):4339–4348. [PubMed: 16618759]
18. Orlova A, Magnusson M, Eriksson TL, Nilsson M, Larsson B, Hoiden-Guthenberg I, Widstrom C, Carlsson J, Tolmachev V, Stahl S, Nilsson FY. Cancer research. 2006; 66(8):4339–4348. [PubMed: 16618759]

$watermark-text

$watermark-text

$watermark-text

19. Vittaz M, Bazile D, Spenlehauer G, Verrecchia T, Veillard M, Puisieux F, Labarre D. Biomaterials. 1996; 17(16):1575–1581. [PubMed: 8842361]
20. Romberg B, Hennink WE, Storm G. Pharm Res. 2007
21. Romberg B, Hennink WE, Storm G. Pharmaceutical research. 2008; 25(1):55–71. [PubMed: 17551809]
22. Cheng J, Teply BA, Sherifi I, Sung J, Luther G, Gu FX, Levy-Nissenbaum E, Radovic-Moreno AF, Langer R, Farokhzad OC. Biomaterials. 2007; 28(5):869–876. [PubMed: 17055572]
23. Friedman M, Nordberg E, Hoiden-Guthenberg I, Brismar H, Adams GP, Nilsson FY, Carlsson J, Stahl S. Protein Eng Des Sel. 2007; 20(4):189–199. [PubMed: 17452435]
24. Orlova A, Tolmachev V, Pehrson R, et al. Cancer Res. 2007; 67(5):2178–2186. [PubMed: 17332348]
25. Tolmachev V, Orlova A, Nilsson FY, Feldwisch J, Wennborg A, Abrahmsen L. Expert opinion on biological therapy. 2007; 7(4):555–568. [PubMed: 17373906]
26. Orlova A, Tolmachev V, Pehrson R, Lindborg M, Tran T, Sandstrom M, Nilsson FY, Wennborg A, Abrahmsen L, Feldwisch J. Cancer research. 2007; 67(5):2178–2186. [PubMed: 17332348]
27. Maier L, Xu FJ, Hester S, et al. Cancer Res. 1991; 51(19):5361–5369. [PubMed: 1680547]
28. Maier LA, Xu FJ, Hester S, Boyer CM, McKenzie S, Bruskin AM, Argon Y, Bast RC Jr. Cancer research. 1991; 51(19):5361–5369. [PubMed: 1680547]
29. Ruoslahti E. Annual review of cell and developmental biology. 1996; 12:697–715.
30. Zhang L, Radovic-Moreno AF, Alexis F, Gu FX, Basto PA, Bagalkot V, Jon S, Langer RS, Farokhzad OC. ChemMedChem. 2007; 2(9):1268–1271. [PubMed: 17600796]
31. Farokhzad OC, Cheng J, Teply BA, Sherifi I, Jon S, Kantoff PW, Richie JP, Langer R. Proceedings of the National Academy of Sciences of the United States of America. 2006; 103(16): 6315–6320. [PubMed: 16606824]
32. Farokhzad OC, Jon S, Khademhosseini A, Tran TN, Lavan DA, Langer R. Cancer research. 2004; 64(21):7668–7672. [PubMed: 15520166]
33. Gu F, Zhang L, Teply BA, Mann N, Wang A, Radovic-Moreno AF, Langer R, Farokhzad OC. Proceedings of the National Academy of Sciences of the United States of America. 2008; 105(7): 2586–2591. [PubMed: 18272481]

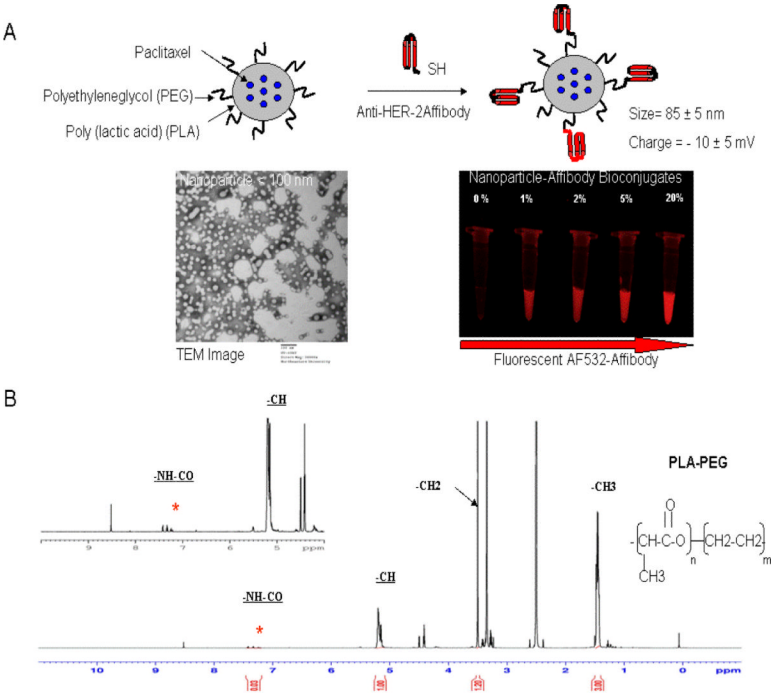

Figure 1.

A) Schematic diagram of the formation of drug encapsulated PLA-PEG-Mal nanoparticle-Affibody bioconjugates. Nanoparticle's size diameter (< 100 nm) and distribution was visualized by electron microscopy. The hydrophilic polyethyleneglycol (PEG) chains on the surface reduce the protein absorption on the hydrophobic polymeric surface to form "stealth" nanoparticles. Direct visualization of Affibody conjugation on the surface of the nanoparticle was carried out using fluorescent image of fluorescent Affibody (Alexa Fluor 532; *red*) conjugated to nanoparticles. After washing the nanoparticle-Affibody bioconjugates, the fluorescent signal increases with an increased amount of fluorescent Affibody (0-20 % Affibody/polymer molar ratio) on the nanoparticle surface confirming the chemical conjugation efficiency. **B)** ^{1}H-NMR (proton nuclear magnetic resonance) spectrum represents the PLA-PEG-Affibody bioconjugates. The ^{1}H-NMR spectrum shows the protons assigned to the polymer (δ = 1-6 ppm) and the presence of Affibody polypeptide (δ = 7-8 ppm) confirming the chemical conjugation of the Affibody on the polymeric nanoparticles.

$watermark-text
$watermark-text
$watermark-text

$watermark-text

$watermark-text

$watermark-text

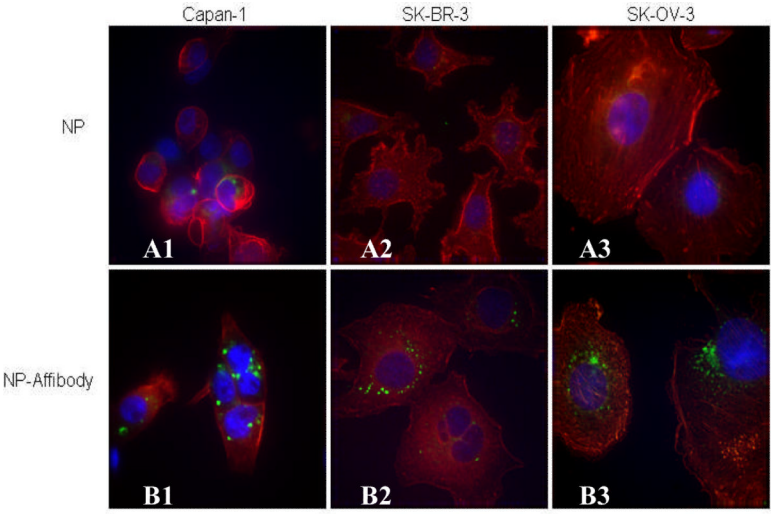

Figure 2.

Fluorescent microscopy of nanoparticle-Affibody bioconjugates incubated with HER-2 positive cell lines. Capan-1 cells, SK-BR-3 cells and SK-OV-3 cells were grown on chamber slides and incubated in OptiMEM medium supplemented with 5 μg of NBD fluorescent dye encapsulated into nanoparticles shown in green with (upper panel) or targeted nanoparticle-Affibody bioconjugates (lower panel) for 2 hours prior imaging using fluorescent microscopy at 60X magnification. The cell nuclei and the actin cytoskeleton are stained with *blue* (4',6-diamidino-2-phenylindole) and *red* (Alexa-Flour Phalloidin-488), respectively. The deconvoluted fluorescent images represent the mid-cross section of the cells after washing (3 times), permeabilizing and staining steps.

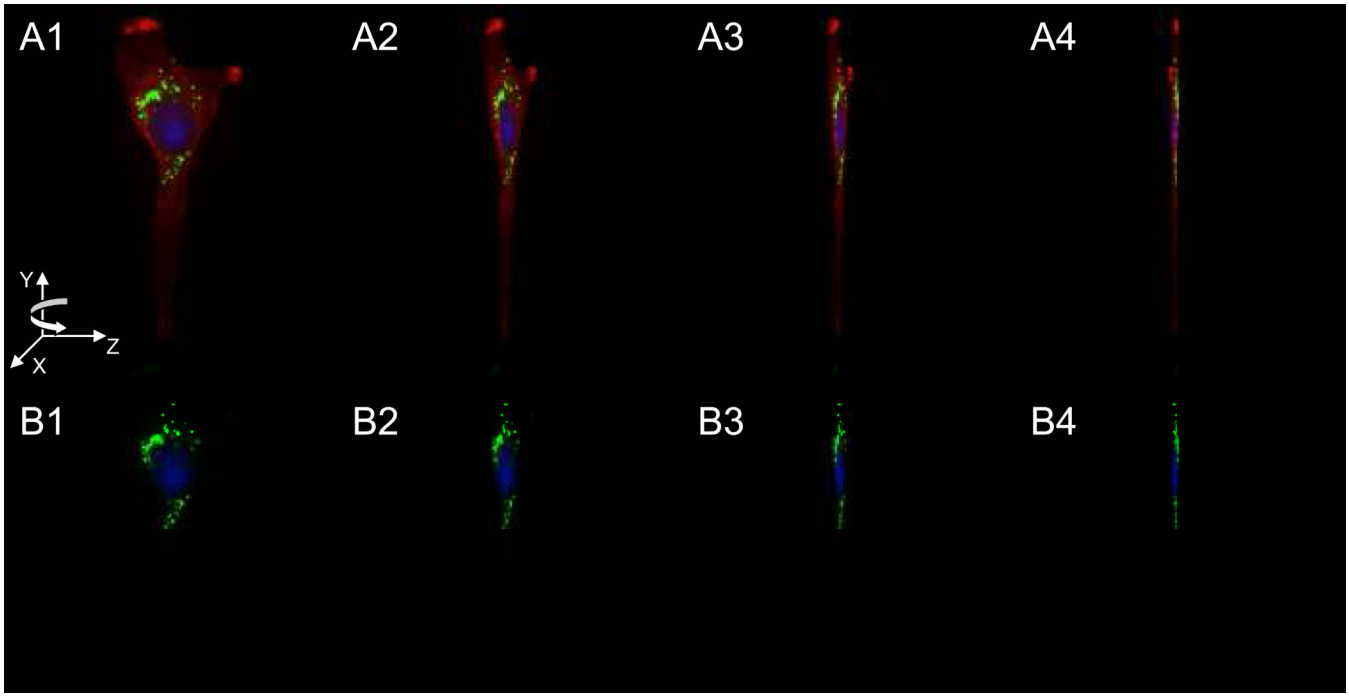

Figure 3.
Combined fluorescent images (60X magnification) of a single SK-BR-3 cell to reconstruct a three-dimensional image of the cell. A1-A4 (upper panel) images represent the mid-cross section images of the same SK-BR-3 cell being rotated at 30-degree intervals along the y-axis. A4 represents an image of SK-BR-3 rotated to 90-degree along the y-axis demonstrating particles shown in *green* (NBD fluorescent dye encapsulated into the nanoparticles) internalized inside the cell. The cell nuclei and the actin cytoskeleton are stained with *blue* (4',6-diamidino-2-phenylindole) and *red* (Alexa-Flour Phalloidin-488), respectively. B1-B4 (lower panel) represents fluorescent images of the same SK-BR-3 (shown in the upper panel) cell without the actin cytoskeleton staining confirming the internalization of the nanoparticle-Affibody bioconjugates inside the cell.

$watermark-text
$watermark-text
$watermark-text

$watermark-text
$watermark-text
$watermark-text

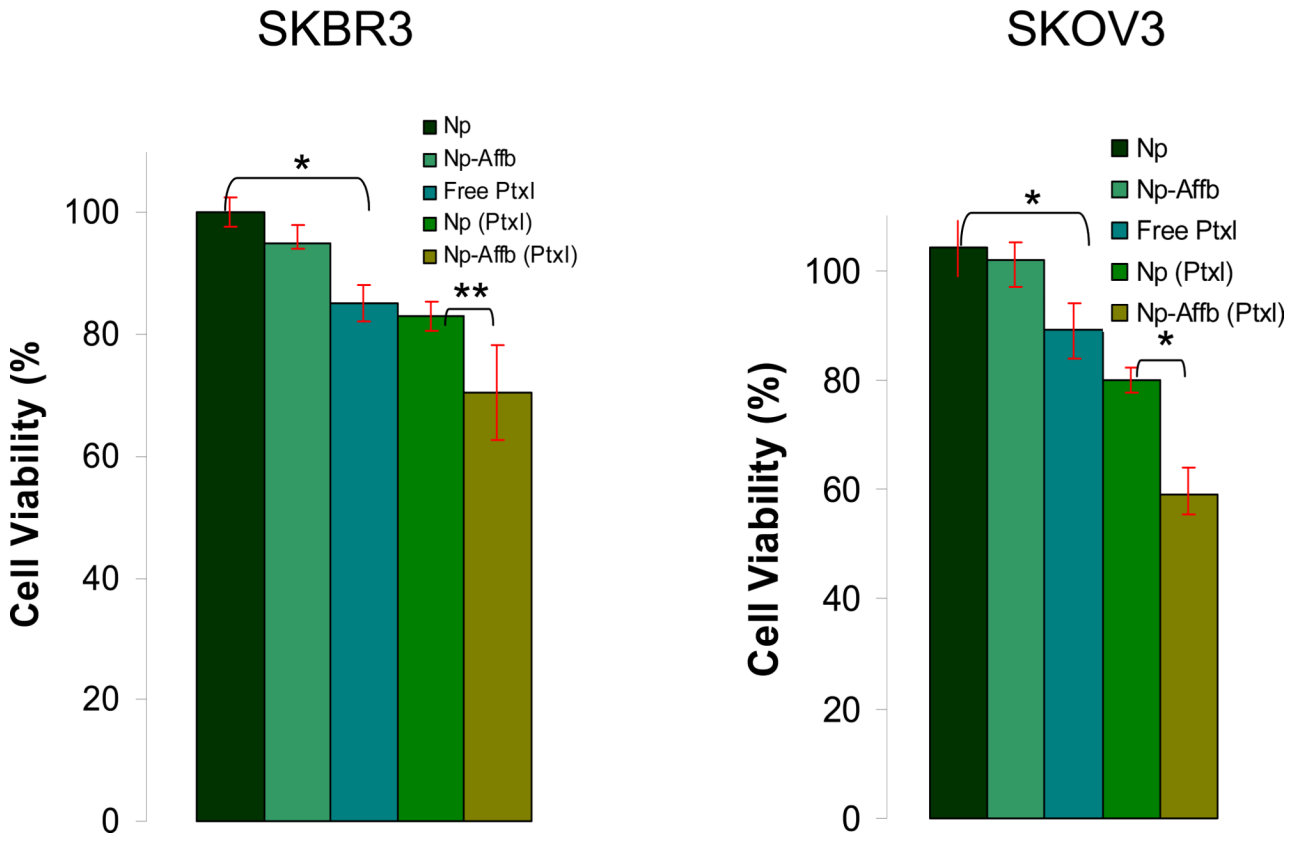

Figure 4.

Cell viability assay (MTS assay) to evaluate the differential toxicity of targeted (Np-Affb) and untargeted nanoparticles (Np) with and without encapsulated paclitaxel (Ptxl). In this assay, the nanoparticle formulations were incubated for 2 hours, cells were subsequently washed and incubated in cell growth media to allow the effect of the drug on the cell cycles before quantifying the nanoparticle formulations toxicities against two cancer cell lines expressing HER-2 (SK-BR-3 and SK-OV-3).ANNOVA test ”*” $p<0.01$; “**” $p<0.05$.